

Linköping University Post Print

**Phase Based Level Set Segmentation of Blood
Vessels**

Gunnar Låthén, Jimmy Jonasson and Magnus Borga

N.B.: When citing this work, cite the original article.

©2009 IEEE. Personal use of this material is permitted. However, permission to reprint/republish this material for advertising or promotional purposes or for creating new collective works for resale or redistribution to servers or lists, or to reuse any copyrighted component of this work in other works must be obtained from the IEEE:

Gunnar Låthén, Jimmy Jonasson and Magnus Borga, Phase Based Level Set Segmentation of Blood Vessels, 2008, Proceedings of 19th International Conference on Pattern Recognition.
<http://dx.doi.org/10.1109/ICPR.2008.4760970>

Postprint available at: Linköping University Electronic Press
<http://urn.kb.se/resolve?urn=urn:nbn:se:liu:diva-21054>

Phase Based Level Set Segmentation of Blood Vessels

Gunnar L  th  n

*Department of Science and Technology
Link  ping University*

Jimmy Jonasson

*Department of Biomedical Engineering
Link  ping University*

Magnus Borga

*Department of Biomedical Engineering and
Center for Medical Image Science and Visualization
Link  ping University*

Abstract

The segmentation and analysis of blood vessels has received much attention in the research community. The results aid numerous applications for diagnosis and treatment of vascular diseases. Here we use level set propagation with local phase information to capture the boundaries of vessels. The basic notion is that local phase, extracted using quadrature filters, allows us to distinguish between lines and edges in an image. Noting that vessels appear either as lines or edge pairs, we integrate multiple scales and capture information about vessels of varying width. The outcome is a ‘‘global’’ phase which can be used to drive a contour robustly towards the vessel edges. We show promising results in 2D and 3D. Comparison with a related method gives similar or even better results and at a computational cost several orders of magnitude less. Even with very sparse initializations, our method captures a large portion of the vessel tree.

1. Introduction

A correct segmentation of blood vessels is of major importance in many medical applications, e.g. diagnosis, surgical planning, simulation and training. It is well accepted that there is no general purpose segmentation method suitable for all applications and imaging modalities. As such, the problem has been approached from many disciplines using many different methods. Roughly, the techniques either segment the vessel centerlines (skeleton based) or the vessel boundaries (non-skeleton based). The basic challenges that all vessel segmentation methods tackle are varying vessel width, bifurcations and changing contrast. We refer the reader

to [8, 2] for more complete reviews of previous work.

For our method we use the fact that vessels of different widths all can be perceived as lines or edge pairs, depending on the scale on which they are observed. Thus, it is possible to use a line detector incorporating multiple scales as previously demonstrated by [3]. Our approach extends this idea by also including edge detection. Furthermore, rather than using multiple scales purely for noise reduction, we accumulate both line and edge information across all scales, maximizing the amount of information extracted. The core of our method is the use of quadrature filters and local phase as a line/edge detector which will be further elaborated in Section 2. In comparison to gradient-based edge detectors, local phase gives well defined vessel boundaries even for poor contrast. This leads to robust convergence when combined with front propagation methods for segmentation, as will be outlined in Section 3. To verify our results we use the DRIVE database of retinal images [7] in 2D and angiogram images generated by magnetic resonance (MRA) in 3D.

To summarize, our main contribution is the use of quadrature filters and local phase in a multi-scale setting producing global information usable for segmenting vessels of varying width and contrast. Local phase has been used for live-wire segmentation in [4], but to the best of our knowledge, the use of local phase as a driving force for propagating fronts is a novel idea.

2. Quadrature filters

A quadrature filter is zero over one half of the Fourier domain, as defined by:

$$F_k(\mathbf{u}) = 0, \quad \mathbf{u} \cdot \mathbf{n}_k \leq 0 \quad (1)$$

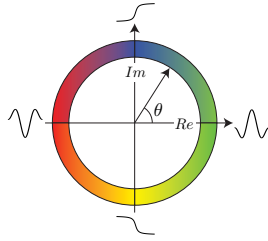


Figure 1. Local phase

where u is frequency and n_k the filter direction. In practice, the filter is implemented as a complex valued filter pair consisting of a line filter as real part and an edge filter as imaginary part [1]. Thus, when the filter response is purely real, the filtered signal is strongly “line-like”, whereas a purely imaginary response indicates an “edge-like” signal. The magnitude of the filter response gives the strength of the structure, while the angle of the response indicates the type of structure (line/edge). The angle θ is referred to as the *local phase*, illustrated in Figure 1 along with the color mapping used in remaining illustrations. Since θ is independent of signal strength, the local phase as a line/edge detector is invariant to image contrast, making it an appealing and more robust alternative to gradient-based edge detectors.

2.1. Combining filter directions

In practice, an image is filtered in at least 3 uniformly distributed directions in 2D and 6 directions in 3D to capture structure of all orientations. Thus, the local phase is a characteristic along particular directions. To produce a rotation invariant phase map, the filter responses from all orientations need to be combined. However, the different filter directions introduce an ambiguity. Consider a vertical edge. A filter with dominant direction along the positive real axis approaches this edge from the left, giving a phase tending to 90° . On the contrary, a filter with dominant direction along the negative real axis will approach it from the right, giving a phase tending to -90° . This will produce cancellation effects and discontinuities in the combined phase map. The solution is to compute the orientation of the dominant structure at each point, and flip the phase along the real axis for a filter with direction opposing the orientation. This will produce the same phase response for an edge independent of filter direction. When this ambiguity has been resolved, a rotation invariant phase map is produced by summing the filter responses for all directions.

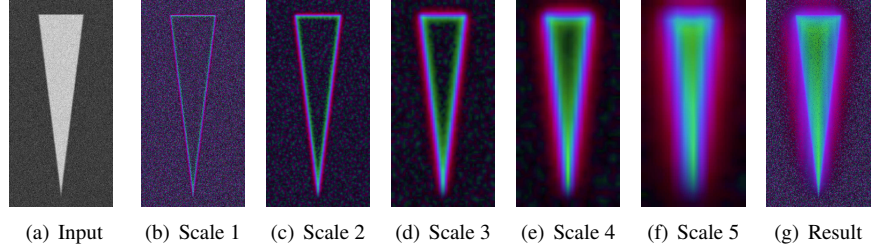


Figure 2. Filter across increasing scales

2.2. Multi-scale integration

The core idea behind our method is to use the fact that vessels of different width appear both as lines and edges across different scales. In order to produce a *global phase* map used for segmentation, we want to combine the different scales. We achieve this by a weighted sum over all scales, such that high strength responses are favored. This is expressed as:

$$q = \frac{\sum_{i=1}^N |q_i|^\beta q_i}{\sum_{i=1}^N |q_i|^\beta} \quad (2)$$

where N is the number of scales, q_i is the combined filter response for each scale and β is a weight parameter. To illustrate this, we use a synthetic “wedge” image (see Figure 2(a)) which displays a large width variation. The filtering of 5 scales and integration using a typical value of $\beta = 1$ are shown in Figure 2. Note that the result contains detailed information about both line and edge structures. As a final processing step, we apply normalization to the output magnitude by:

$$\hat{a}(\sigma) = 1/(1 + (\sigma/a)^2) \quad (3)$$

where $a = |q|$, q is the global phase map and σ is a data dependent threshold parameter. This normalization removes scaling issues associated with different inputs, so σ should be viewed as a replacement for more complicated parameters compensating for scaling. Currently, σ is set manually, but can be automatically computed based on analysis of the noise.

3. Level set methods and front propagation

From the previous section, we can conclude that edges produce a phase of 90° , which means that edges align with the zero-crossings of the *real part* of the phase map. The phase based edge detector has a major advantage compared to other common gradient-based edge detectors. Briefly, edge detectors based on gradients are typically formulated as $g(\mathbf{x}) = 1/(1 + |\nabla I|^2)$

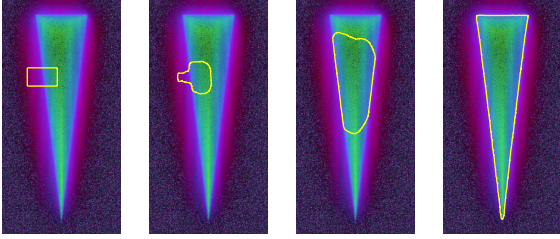


Figure 3. Sequence of iterations

where I is the input image. The idea is that $g(\mathbf{x})$ approaches zero when the gradient magnitude is large. Using front propagation techniques, this is often used as a “switch” to halt propagation near edges. However, a common problem is leakage since $g(\mathbf{x}) > 0$ for realistic situations. Using phase based edge detectors on the other hand, gives very robust convergence to edges since they are located on a well defined zero-crossing.

In our work we use the popular level set method [5] as a means for front propagation. This technique represents the front, or contour, implicitly as the zero level set of a time dependent signed distance function $\phi(\mathbf{x}(t), t)$, i.e. $\{\mathbf{x}(t) : \phi(\mathbf{x}(t), t) = 0\}$. Equations of motion can be derived by differentiating ϕ w.r.t. time. This framework for deforming contours has two major advantages: Topological changes are handled naturally (as opposed to explicit/parametric representations) and it allows for non-monotonic motion (as opposed to the fast marching method [6]).

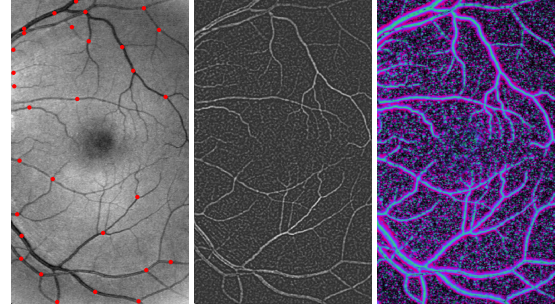
Relating this to the phase based edge detector, our idea is to use the real part of the phase map as a speed function to drive a deforming contour. We add a curvature-based term for regularization, giving the evolution equation:

$$\frac{\partial \phi}{\partial t} = -\text{Re}(\hat{q}(\sigma)) |\nabla \phi| + \alpha \kappa |\nabla \phi| \quad (4)$$

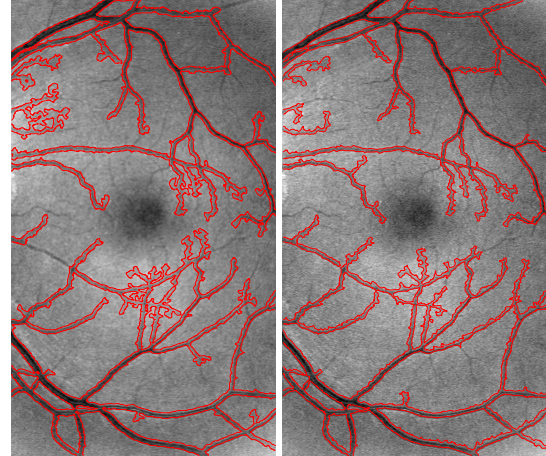
where \hat{q} denotes the normalized phase map by Eq. (3), α is a regularisation parameter and κ is curvature (mean curvature in 3D). A sequence of iterations using this speed function is displayed in Figure 3.

4. Experiments

We implemented the proposed method in Matlab. The level set framework is standard using narrow band computations and either PDE-based or fast marching-based reinitialization. The code can be found online at <http://dmforge.itn.liu.se/icpr08/> for reference. For comparison we implemented the “Flux Maximizing Flow” (FMF) [9] which has been proven as a robust alternative to gradient-based segmentation. This



(a) Input image and manual seeds (b) FMF speed function (c) Phase map speed function



(d) FMF results (e) Phase map results

Figure 4. Segmentation result in 2D

approach is similar to ours in the sense that it views vessels at different scales and generates a speed function where vessel boundaries are located on zero-crossings. Thus, the same level set propagation tool can be used.

For our first experiment in 2D, we used a 458×265 retinal image from the DRIVE database [7] displayed in Figure 4(a). The speed functions generated by FMF and our method are shown in Figure 4(b) and Figure 4(c). For the phase map speed function we used 4 filters of size 15×15 with bandwidths of 4 octaves and center frequencies of $5\pi/7$. We used 3 scales by subsampling the image twice with a factor of $1/\sqrt{2}$. A typical value of $\beta = 1$ was used for the scale integration (Eq. (2)). For Eq. (4), we set the normalization parameter σ to 3 and the regularization parameter α to 0.005 for both methods. We initialized using manual seeds as depicted in Figure 4(a) and executed both algorithms until convergence, which was defined as the total change of the contour being less than 25 pixels between two time-steps.

To show the extension of our method to 3D, we used the $416 \times 512 \times 112$ “Head MRT Angiography” sample dataset from www.volvis.org, displayed as a MIP in

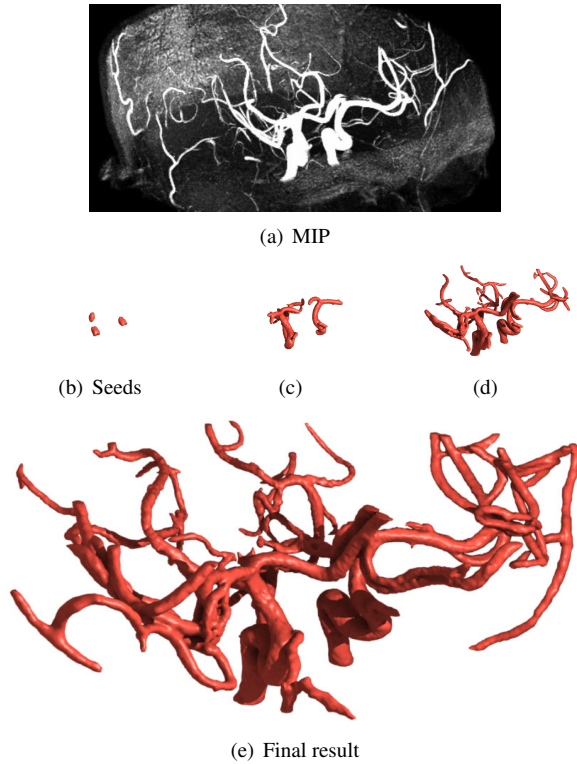


Figure 5. Segmentation results in 3D

Figure 5(a). For this experiment we used 6 filters of size $7 \times 7 \times 7$ with bandwidths of 6 octaves and center frequencies of $\pi/2$. We used 2 scales with ratio of 2 and the parameter values $\beta = 1$, $\sigma = 150$ and $\alpha = 0.03$ for Eq. (2) and Eq. (4). We set manual seeds as depicted in Figure 5(b).

5. Results

For optimized parameter settings for FMF and the proposed method, we can in Figure 4 note that our approach exhibits less leakage, indicating more robust convergence. Furthermore, the execution time to generate the speed functions differs by several orders of magnitude in favor of our filter-based method (31 minutes vs. 1.9 seconds). For the 3D experiment in Figure 5(e), we manually initialized with 3 seeds in large vessels to display the ability to grow a large portion of the vessel tree given sparse initialization.

6. Discussion and future work

We have presented an approach for segmenting blood vessels using multi-scale integration of local phase combined with level set propagation. We show

proof-of-concept examples in 2D and 3D, displaying the effectiveness of the method. When using front propagation techniques, stable convergence is relying on “inside” and “outside” forces around the vessel boundaries to balance, and experience yields that our method has stronger “outside” forces compared to the FMF method. Furthermore, experiments show that the computational efforts in generating the speed function for propagation is very low using our method. We have not spent any efforts on optimizing our implementations with respect to computational cost, but optimization alone cannot reduce the complexity of the FMF algorithm to a comparable simplicity level and execution time. We are aware of the common problem that mean curvature regularisation removes thin vessels, but the strong filter response from the line structures counteracts these effects for our method. The current results are proof-of-concept and we acknowledge the need for more quantitative and qualitative comparisons to other current methods and different types of data. In addition, future work includes regularization of the filter output and development of more optimal filters.

References

- [1] G. H. Granlund and H. Knutsson. *Signal Processing for Computer Vision*. Kluwer Academic Publishers, Netherlands, 1995.
- [2] C. Kirbas and F. Quek. A review of vessel extraction techniques and algorithms. *ACM Comput. Surv.*, 36(2):81–121, 2004.
- [3] Q. Li, J. You, L. Zhang, D. Zhang, and P. Bhattacharya. A new approach to automated retinal vessel segmentation using multiscale analysis. In *ICPR*, volume 4, pages 77–80, 2006.
- [4] L. O’Donnell, C.-F. Westin, W. E. L. Grimson, J. Ruiz-Alzola, M. E. Shenton, and R. Kikinis. Phase-based user-steered image segmentation. In *MICCAI ’01*, pages 1022–1030, London, UK, 2001. Springer-Verlag.
- [5] S. Osher and J. A. Sethian. Fronts propagating with curvature-dependent speed: Algorithms based on Hamilton-Jacobi formulations. *Journal of Computational Physics*, 79:12–49, 1988.
- [6] J. Sethian. A fast marching level set method for monotonically advancing fronts. In *PNAS*, volume 93, pages 1591–1595, 1996.
- [7] J. Staal, M. Abramoff, M. Niemeijer, M. Viergever, and B. van Ginneken. Ridge based vessel segmentation in color images of the retina. *IEEE Transactions on Medical Imaging*, 23(4):501–509, 2004.
- [8] J. S. Suri, K. Liu, L. Reden, and S. Laxminarayan. A review on mr vascular image processing: skeleton versus nonskeleton approaches: part ii. *IEEE Trans Inf Technol Biomed*, 6(4):338–350, 2002.
- [9] A. Vasilevskiy and K. Siddiqi. Flux maximizing geometric flows. *IEEE Trans. Pattern Anal. Mach. Intell.*, 24(12):1565–1578, 2002.